ELSEVIER

Journal of Fluorine Chemistry 73 (1995) 137–146

JOURNAL OF FLUORINE CHEMISTRY

Thermal decomposition reactions of gaseous dioxygen difluoride and dioxygen fluoride at ambient temperature

K.D. Abney [a,*], P.G. Eller [a], M.P. Eastman [b], C.F. Pace [a], S.A. Kinkead [a], R.J. Kissane [a], W.H. Woodruff [a]

[a] *Isotope and Nuclear Chemistry Division, Los Alamos National Laboratory, Los Alamos, NM 87545, USA*
[b] *Department of Chemistry, Northern Arizona University, Flagstaff, AZ 86011, USA*

Received 2 September 1993; accepted 19 December 1994

Abstract

The decomposition of gaseous dioxygen difluoride (FOOF) and dioxygen fluoride (FOO) to F_2 and O_2 at ambient temperature has been studied by electron paramagnetic resonance (EPR) spectroscopy, Fourier-transform infrared (FT-IR) spectroscopy and transient gas pressure measurements. The formation of oxygen in FOOF/FOO gas mixtures, as demonstrated by stopped-flow EPR, was first-order under low-pressure conditions (1–10 Torr) with rate constants in the range of 0.1–0.2 s^{-1}, depending upon wall materials. EPR spectroscopy detected neither F atoms nor FOO radicals as intermediates despite the presence of FOO radicals shown by complementary FT-IR experiments. The FT-IR spectra of gaseous FOOF undergoing decomposition at ambient temperature showed prominent, isolated bands near 1210 cm^{-1} (FOOF) and near 1490 cm^{-1} (FOO). Overlapping bands attributable to both species were seen near 650 cm^{-1}, and weak features appeared elsewhere. At nominal initial FOOF/FOO pressures of 4–20 Torr, results from stopped-flow FT-IR kinetics analysis using these bands generally agreed with the EPR results and yielded first-order rate constants of 0.12 ± 0.01 s^{-1} and 0.22 ± 0.03 s^{-1}, respectively, for FOO and FOOF disappearance. Oxygen-carrier FT-IR experiments strongly suggested that a reversible reaction between FOOF and O_2 forms FOO ($K_{eq} \approx 0.018$), and that this reaction was rapid relative to FOOF/FOO decomposition. Analysis of the stopped-flow FT-IR results yielded infrared peak absorptivities for FOOF absorption at 1205 cm^{-1} of $1.8 \pm 0.4 \times 10^{-3}$ (Torr cm)$^{-1}$ and for FOO absorption at 1486 cm^{-1} of $3.5 \pm 1 \times 10^{-3}$ (Torr cm)$^{-1}$. The observed kinetics are discussed in terms of the possible decomposition reaction mechanisms.

Keywords: Thermal decomposition reactions; Dioxygen difluoride; Dioxygen fluoride; IR spectroscopy; EPR spectroscopy

1. Introduction

Dioxygen difluoride (FOOF) is one of the most potent of all known fluorinating agents; its reactivity at ambient temperature is matched only by elemental fluorine at temperatures hundreds of degrees Kelvin above ambient [1,2]. This compound is thermally unstable and decomposes to $O_2(g)$ and $F_2(g)$, a property that explains its extreme fluorinating power. Although FOOF has been studied for about 50 years, its reactivity and unusual structural and spectroscopic features are still incompletely understood and are the subject of other investigations [3–6].

Within the past eight years, research has shown that the dioxygen fluoride radical (FOO) is a prominent species during the decomposition of gaseous FOOF [5,6]. Like FOOF, FOO is a thermodynamically unstable, powerful fluorinating agent with an ambient temperature lifetime of a few seconds. Because previously published studies were limited in scope and failed to recognize the importance of FOO or were complicated by side-reactions, we do not have a quantitative understanding of the thermal stability of FOOF/FOO mixtures and the role of FOO in the decomposition of FOOF [2,5–8]. In addition, the lack of convenient large-scale syntheses and rapid diagnostic techniques has greatly hindered kinetic studies of these highly unstable and reactive materials. Dramatic advances in these areas and in handling procedures have significantly alleviated the above difficulties [3–6,10] [1].

* Corresponding author.

[1] Dioxygen difluoride has also been prepared thermally by circulating a 1:1 oxygen/fluorine mixture through a heated (≈ 850 °C) nickel tube to dissociate the fluorine and trapping the FOOF product in a liquid-nitrogen-cooled copper block reservoir. The reservoir was then allowed to warm up slowly in order to transfer the FOOF dynamically to the liquid-nitrogen-cooled storage vessel [9].

Elsevier Science S.A.
SSDI 0022-1139(95)03230-4

The overall gas-phase decomposition of FOOF is described by the following simple net reaction:

$$FOOF_{(g)} \longrightarrow F_{2\,(g)} + O_{2\,(g)} \quad (1)$$

Appreciable quantities of FOO coexist with decomposing gaseous FOOF [5,6]. As observed for FOOF, overall decomposition of FOO to its constituent elements also occurs and must be taken into account in kinetic analyses:

$$FOO_{(g)} \longrightarrow 1/2F_{2\,(g)} + O_{2\,(g)} \quad (2)$$

Several of the microscopic mechanisms for reactions (1) and (2) are direct unimolecular decomposition to O_2 and F_2, unimolecular dissociation of FOOF to FOO and F followed by rapid reactions to produce O_2 and F_2, bimolecular pathways initiated by collisions between FOOF (or FOO) molecules and decomposition pathways involving collisions between FOOF molecules and cell walls or diluent gas molecules. Possible reaction pathways involving equilibria between FOOF, O_2 and FOO must also be considered.

Several studies have reported the use of in situ photolysis of O_2/F_2 gas mixtures to examine the formation and decomposition kinetics of FOOF/FOO mixtures at ambient and sub-ambient temperatures [5,6]. In these experiments, the FOOF/FOO concentrations were low and wall reactions relatively unimportant. An earlier study used a closely related but much more restrictive photolytic approach [7]. In several previous kinetics investigations, 'batch' FOOF decomposition was studied at sub-ambient temperatures and low pressures [2,5,8].

In our present study we have determined the decomposition rates of gaseous FOOF and FOO at ambient temperature and pressures relevant to large-scale synthesis to (a) assess the relative roles of heterogeneous decomposition at surfaces and homogeneous gas-phase reactions in determining FOOF and FOO stabilities and (b) infer possible mechanism(s) of decomposition under conditions relevant to chemical applications. In the process, we have redetermined molar absorptivities and oscillator strengths for the major infrared absorption bands at 1486 cm^{-1} (FOO) and 1205 cm^{-1} (FOOF) and have confirmed that the reaction of FOOF and O_2 yielding FOO is rapid and reversible at ambient temperature. These results are important for understanding the unusual reactivity and spectroscopic properties of these extremely strong oxidants and for optimizing chemical schemes that take advantage of their unique properties.

2. Experimental details

2.1. Physical methods and data collection

Danger: *Because dioxygen difluoride is one of the most powerful of all known oxidative fluorinating agents, it can initiate extremely violent reactions. It is not shock-sensitive; however, explosive pressure rises may occur during its decomposition.*

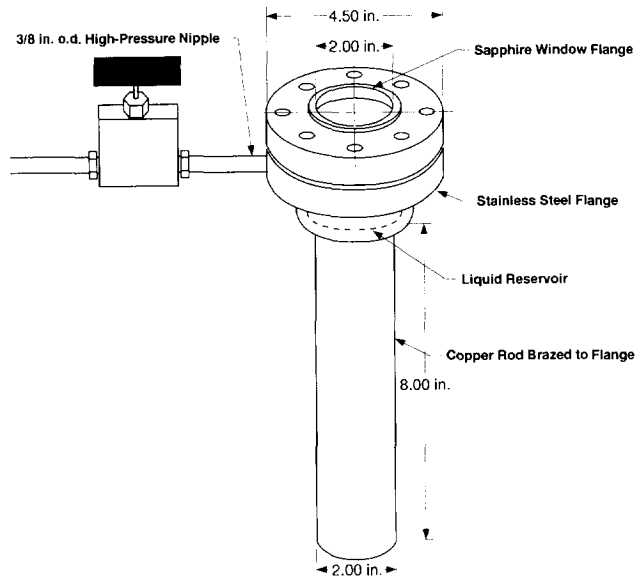

Fig. 1. Schematic diagram of apparatus used for the photochemical synthesis of FOOF.

Dioxygen difluoride, prepared in 5–30 g batches by both photochemical and thermal methods [9], was stored in well-passivated stainless-steel containers at liquid nitrogen temperature until needed. Photochemical synthesis was performed in an apparatus (Fig. 1) consisting of a 4.5 in stainless-steel flange bottom with a small liquid reservoir connected by a copper gasket to a 2 in sapphire window that was mounted on a 4.5 in flange (MDC Manufacturing, Inc.) [10]. A quartz plate heat shield was used between the lamp and the sapphire window, and the space between the windows was purged with helium to prevent frosting. An 8 in copper rod was soldered to the lower flange to cool the assembly in liquid nitrogen. In a typical preparation, fluorine (1500 Torr) and oxygen (1500 Torr) were admitted into 1 l ballast cans that were attached to a metal vacuum line. The contents of these cans were condensed into the reactor by raising a liquid-nitrogen-filled Dewar to the level of the sapphire window.

Caution: *Pressure on the sapphire window of the reactor should never exceed atmospheric pressure.*

Ultraviolet light from a high-pressure 1000 W Hg/Xe lamp was focused into the reactor and onto the liquid F_2/O_2 mixture for 2–3 h while the liquid nitrogen level was kept constant. The FOOF froze in the cold reactor; after irradiation, the residual gas was pumped away at − 196 °C, leaving the FOOF product as a red–orange solid. The liquid-nitrogen-filled Dewar was carefully lowered to allow the reactor to warm slowly while the volatilized FOOF product was transferred dynamically to a liquid-nitrogen-cooled storage can. A yield of 5–6 g (80%–90%) was typical for this type of preparation.

Electron paramagnetic resonance (EPR) spectra were recorded on an IBM ER 200D X-band spectrometer equipped with an ER 4102 ST cavity operating at a field modulation frequency of 100 MHz. In both the continuous-flow and stopped-flow experiments, the spectrometer was operated

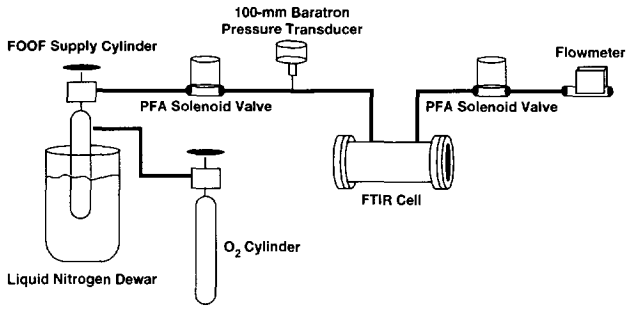

Fig. 2. Schematic diagram of the FT-IR stopped-flow system employed in the FOOF/FOO decomposition experiments.

with the power incident on the cavity at 2 mW or less. Bomem DA3.002 and Nicolet 20SX spectrometers were used for Fourier-transform infrared (FT-IR) measurements at 4 cm^{-1} resolution. In the FT-IR kinetic experiments, the infrared cell (12.5 cm pathlength and 3.5 cm diameter) had stainless-steel walls and AgCl windows. The oxygen carrier experiments employed both stainless steel and Monel cells fitted with AgCl windows. All experiments were conducted at ambient temperature (297 ± 3 K).

Fig. 2 presents a schematic diagram of the stopped-flow system used for the FT-IR experiments. For kinetic observations, the gs flow could be stopped rapidly (0.2 s cycle speed) by simultaneously closing the perfluoroalkoxy (Teflon® PFA)-coated solenoid valves on either side of the observation cell. The volume of the infrared cell represented $\approx 85\%$ of the total volume of the kinetic system isolated by the solenoid valves. Thus, the observed spectroscopic changes caused by decomposition and the derived kinetics were predominantly the result of reactions that occurred within the volume of the infrared cell itself.

In a typical FT-IR kinetics run, the position of the liquid-nitrogen-filled Dewar that cooled the FOOF supply cylinder was adjusted until the desired dynamic pressure (as measured by MKS Baratron® pressure transducers) was produced in the flow system. Flow rates were monitored with a Teledyne–Hastings mass-flow transducer. The infrared spectrum of the flowing gas was monitored until byproducts (notably CF_4) produced in the original FOOF synthesis or by the reaction of FOOF with flow system impurities were virtually unobservable. Single-scan interferograms were collected at a maximum rate of three per second while FOOF was flowing through the cell. After several interferograms had been collected, the solenoid valves were closed: additional interferograms were recorded for at least three half-lives after the valves were closed. As the FT-IR data were collected, the time-dependence of the pressure rise caused by FOOF/FOO decomposition was measured and plotted on a fast-response time strip chart recorder.

Oxygen carrier experiments were carried out in two ways. In the first procedure, a bellows pump circulated a mixture of O_2 and F_2 through a flow loop equipped with a photolysis cell upstream from an infrared cell. The photolysis products were observed using the Nicolet 20SX spectrometer. In the second procedure, a single-pass pump-through arrangement used 'batch' FOOF. The FOOF partial pressure was adjusted by varying the level of the Dewar, and the desired O_2 partial pressure was gained from an oxygen cylinder upstream of the FOOF cylinder. Gaseous species were probed in the downstream FT-IR cell.

The infrared spectrum of a flowing FOOF/FOO gas mixture derived from 'batch' FOOF (no carrier gas) is shown in Fig. 3. (A detailed discussion of the absorption features is given in Ref. [11].) Kinetic data were derived from FT-IR experiments by following pressure changes and integrating the FOOF absorption centered near 1210 cm^{-1} from 1140 to 1280 cm^{-1} and the FOO absorption centered near 1490 cm^{-1} from 1450 to 1530 cm^{-1}. This integration procedure also yielded data used to determine oscillator strengths for these bands. Molar extinction coefficients were determined from the FOOF peak maximum at 1205 cm^{-1} and the FOO peak maximum at 1486 cm^{-1} (4 cm^{-1} resolution at total pressures ranging from 3–12 Torr). Because pressure-broadening effects were negligible over this pressure range, given the instrumental resolution indicated peak areas were used to determine kinetic rates. Peak heights could be used to calculate equilibrium concentrations after the molar extinction coefficients had been determined. Care was taken to ensure the absence of fluorocarbons that interfere with the 1210 cm^{-1} band manifold.

The EPR stopped-flow system was essentially identical to that used for the FT-IR measurements (Fig. 2); however, the infrared cell was replaced by a 1 ft section of quartz tubing (10 mm o.d. and 8 mm i.d.) or fluoropolymer (Teflon® FEP) tubing (8 mm o.d. and 6 mm i.d.) that ran directly through the EPR cavity. The stopped-flow valves were removed from the system for continuous-flow EPR experiments.

Kinetic data for O_2 evolution in the decomposition of FOOF/FOO were obtained by following the time-dependence of the total pressure and the amplitude of the EPR oxygen 'E line' [12]. Kinetic analyses using these data must

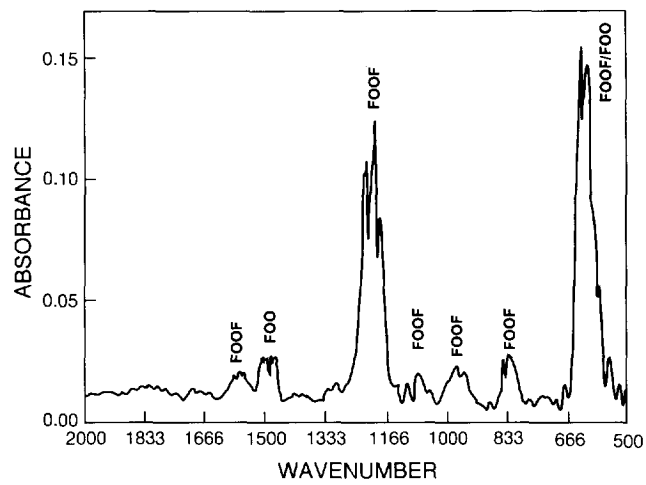

Fig. 3. The infrared spectrum between 2000 and 500 cm^{-1} of a flowing FOOF/FOO gas mixture derived from 'batch' FOOF at 297 K. The nominal FOOF pressure was 12 Torr.

be regarded as approximate because they rely on the assumption that the amplitude of the 'E line' represents an accurate measurement of the change in concentration of oxygen, and therefore this approximation is only valid for relatively small changes in the total pressure. In general, because the oxygen resonance is subject to pressure broadening, a more accurate measure of concentration change is the product of the amplitude and the square of the line width. It was impossible to record simultaneously the line width and the amplitude of the 'E line' in this case because of the relatively rapid rate of the reaction and the limitations of the instrument.

In both the EPR and FT-IR experiments, the reactive gases were discharged through an activated charcoal trap or were allowed to pass directly through the vacuum pump. In some cases, the latter arrangement was preferable (despite the obvious potential hazard and the harsh treatment of the pump) because it resulted in higher flow rates.

3. Results

3.1. Determination of infrared absorption intensities

Stopped-flow FT-IR experiments allow the determination of the molar extinction coefficients for the FOOF and FOO absorption bands even though the absolute concentration of neither species is known. The method used depends on (a) the EPR observation (vide infra) that the concentration of F atoms in the system is very small compared to the combined concentration of FOO and FOOF and (b) the fact that the decomposition of 1 mol of FOOF produces 2 mol of product [reaction (1)], whereas the decomposition of 1 mol of FOO produces 3/2 molof product [reaction (2)]. Thus

$$\Delta P = P^0_{FOOF} + P^0_{FOO}/2 \quad (3)$$

where ΔP is the total pressure rise that occurs after the valves in the stopped-flow system are closed; P^0_{FOOF} and P^0_{FOO} are the partial pressures of FOOF and FOO just before closure of the solenoid valves. For the initial infrared absorbances (A), the cell pathlength (b) and the absorptivities (ϵ), the least-squares expression given by Eq. (4) is obtained:

$$f(\epsilon_{FOOF}, \epsilon_{FOO}) = \sum [\Delta P_i - A_{iFOOF}/(\epsilon_{FOOF} b) - A_{iFOO}/(2\epsilon_{FOO} b)]^2 \quad (4)$$

The summation is over the i data sets for which ΔP, A_{FOOF} and A_{FOO} are available. Minimization of $f(\epsilon_{FOOF}, \epsilon_{FOO})$ with respect to ϵ_{FOOF} and ϵ_{FOO} yields least-squares best-fit values for these two parameters.

For a series of six runs at 296 K with ΔP between 3.2 and 5.9 Torr (Table 1), this approach yielded $\epsilon_{FOOF} = 1.8 \pm 0.4 \times 10^{-3}$ (Torr cm)$^{-1}$ at 1205 cm^{-1} and $\epsilon_{FOO} = 3.5 \pm 1.3 \times 10^{-3}$ (Torr cm)$^{-1}$ at 1486 cm^{-1}. Kim and Campbell reported $\epsilon_{FOOF} = 3.3 \times 10^{-3}$ (Torr cm)$^{-1}$ for the 1210 cm^{-1} FOOF absorption in experiments carried out at 173 K in a long-pathlength FT-IR cell between 50 and 170 mTorr [5]. A value of $\epsilon_{FOO} = 1.2 \times 10^{-3}$ (Torr cm)$^{-1}$ was also reported for the 1490 cm^{-1} FOO band under similar conditions [5]. When the above least-squares procedure was applied to intensities integrated as described in the Experimental section of this paper, oscillator strengths of 22 ± 5 (km mol^{-1}) and 3.0 ± 1 (km mol^{-1}) were obtained for the FOOF and FOO absorptions, respectively. Campbell and coworkers obtained values of 23 km mol^{-1} and 7.9 km mol^{-1}, respectively, at 178 mTorr and 186 K [5].

3.2. EPR experiments

Gas-phase EPR spectroscopy was applied because of the possible involvement of three potentially detectable paramagnetic species (O_2, F and FOO) in the decomposition of FOOF/FOO. Initial efforts focused on detecting the paramagnetic species in a continuous-flow system. In particular, the O_2 resonance is readily observed in flowing FOOF/FOO gas mixtures. Because the intensity of the signal increases in proportion to the length of the section between the FOOF supply and the EPR cavity, the O_2 resonance served as a measure of the extent of end-product O_2 formation by oxygen fluoride decomposition.

Experiments carried out over a range of conditions provided no evidence for a resonance attributable to FOO. Nonlinear triatomic radicals are, in general, difficult to detect in the gas phase by EPR [13]; consequently, even though FOO is readily observed by EPR in condensed media [14] and is easily identified by FT-IR spectroscopy in the gas phase (vide infra), our inability to detect FOO by EPR in the gas phase is not unexpected. In addition, we failed to detect F atoms in flowing FOOF/FOO at total gas pressures between 0.5 and 5 Torr. Fluorine atoms in the gas phase are readily detectable by EPR in systems where F_2 or CF_4 are dissociated by a microwave discharge [15]. We assessed an upper limit on the possible F-atom concentration in our kinetic experiments by determining the sensitivity of our system to F atoms. This measurement employed F atoms that were thermally generated by pumping $F_{2\,(g)}$ at pressures of ≈ 2 Torr through a section of heated nickel tubing which was connected to the EPR cavity by a 0.6 m section of FEP tubing. A temperature of 590 K produced sufficient dissociation of F_2 under these conditions to yield a clear F-atom signal at the positions of the 'C, D and E' lines ($|F,M_F>$ basis, $1,1 \leftrightarrow 1,0$; $2,0 \leftrightarrow 2,-1$; $1,0 \leftrightarrow -1,-1$ transitions) [15]. Calculations using data from the *JANAF Thermochemical Tables* [16] gave $K_p = 1.2 \times 10^{-4}$ (atm$^{1/2}$) at 600 K for the reaction below:

$$1/2F_{2\,(g)} \rightleftharpoons F_{(g)} \quad (5)$$

This corresponds to an $\approx 0.2\%$ dissociation of the fluorine at a total pressure of 2 Torr or, equivalently, a fluorine atom partial pressure of 5×10^{-3} Torr at a total pressure of 2 Torr. We assume this fluorine atom pressure was the maximum (equilibrium) concentration attainable in the heated tube. The actual F-atom concentration in the EPR cavity (downstream in the flow system and at approximately ambient tem-

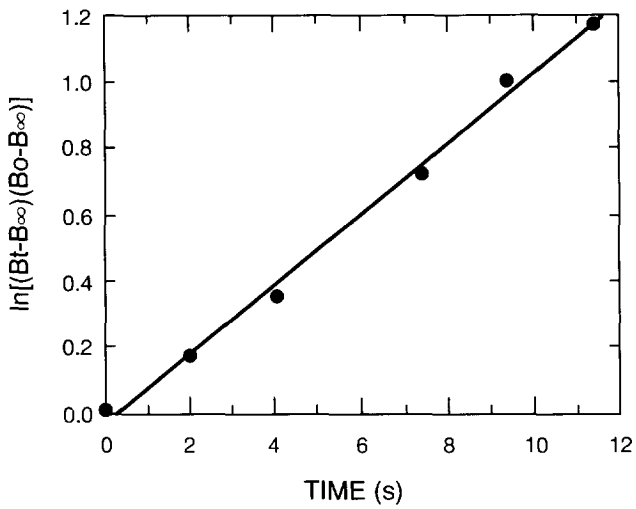

Fig. 4. First-order kinetic plot for oxygen evolution during the decomposition of gaseous FOOF/FOO at ambient temperature. The quantities B_0, B_∞ and B_t represent the EPR amplitudes at $t=0$, $t=\infty$ and at intermediate times. The tubing between the stopped-flow valves was FEP; the initial pressure was 2.14 Torr and the final pressure was 2.58 Torr.

perature) was undoubtedly much lower as a result of F-atom recombination. Thus, for our EPR experiments, the F-atom detection limit must have been lower than 5×10^{-3} Torr of $F_{(g)}$. The failure to observe F atoms implies that either they are not a decomposition intermediate of either FOOF or FOO, as previously suggested [6–8], or they are removed in an extremely efficient manner by reaction with oxygen or by other means and are thus present at concentrations below the EPR detection limit. The latter explanation is the most probable, the rate constant for the reaction of F atoms with O_2 is sufficiently large to account for this result [6].

The infrared experiments described below showed that significant amounts of FOOF and FOO must have been present in the EPR cavity when the valves of the stopped-flow system were closed, as is also shown by the magnitude of the pressure rises. The difference between the final and initial O_2 signals is a measure of undissociated FOOF and FOO in the gas when the flow stopped. The magnitude of the EPR signal at intermediate times likewise indicated the amount of undissociated FOOF/FOO present.

The evolution of O_2 followed first-order kinetics (Fig. 4) over the limited pressure range studied (1–3 Torr). The calculated first-order rate constants are $k=0.11\ s^{-1}$ in FEP and $k=0.21\ s^{-1}$ in quartz. The dependence of the rate constants on total pressure over a greater pressure range was not investigated because of the pressure broadening of the O_2 resonance at higher pressures and difficulties in obtaining reliable EPR and pressure data at very low pressures. The dependence of the rate constants on the type of tubing suggests that under some circumstances wall reactions make a significant contribution to FOOF/FOO decomposition kinetics. Similar wall effects have been reported for F-atom recombination rates [17].

3.3. FT-IR experiments without O_2 carrier gas

Conditions for the EPR and FT-IR experiments differed in several important respects. Because the FT-IR experiments were carried out at higher nominal pressures (higher pumping efficiency) than the EPR experiments, the net transit times between the FOOF supply and spectrometer cell were longer in the EPR runs and consequently a larger fraction of FOOF/FOO had decomposed at $t=0$ in the EPR experiments. The lower pressure and smaller cell diameter in the EPR experiments should also have produced more extensive wall reactions than those in the FT-IR experiments.

Table 1 summarizes pressure data for ambient-temperature stopped-flow FT-IR experiments in which the initial total pressures ranged from 4.2 to 8.5 Torr and the pressure changes ranged from 3.2 to 5.9 Torr. In Fig. 5, the natural logarithms of the integrated areas of the FOOF and FOO peaks have been plotted as a function of time for a typical run in which the initial pressure was 6.60 Torr and the final pressure was 11.24 Torr. This figure also shows that the disappearance of FOOF obeyed good first-order behavior under the conditions employed. An average decomposition rate constant of $0.22\pm0.03\ s^{-1}$ (half-life of 3.2 s) was determined over six runs such as that shown in Fig. 5. Second-order plots clearly exhibited expected deviations from linearity. The data are poorer for FOO and the fit to first- and second-order kinetics was almost equal. A first-order FOO decomposition rate constant of $0.12\pm0.01\ s^{-1}$ (half-life of

Table 1
Pressure and FT-IR kinetic data for FOOF/FOO decomposition at ambient temperature [a]

P_0	ΔP	A_0 (FOOF)	A_0 (FOO)	P_0 (FOOF)	P_0 (FOO)	$P_0(O_2)\simeq P_0(F_2)$	k_{FOOF}	k_{FOO}
4.20	3.20	0.062	0.008	1.65	0.06	1.25	0.22	0.12
4.95	3.50	0.073	0.009	1.95	0.07	1.47	0.17	0.10
6.00	3.80	0.086	0.010	2.28	0.08	1.82	0.26	0.12
6.60	4.64	0.100	0.014	2.67	0.11	1.91	0.22	0.12
6.60	4.60	0.099	0.013	2.63	0.11	1.93	0.25	0.13
8.50	5.90	0.125	0.015	3.34	0.12	2.52	0.21	0.14

[a] The mean first-order decomposition rate constants k_{FOOF} and k_{FOO} were $0.22\pm0.03\ s^{-1}$ ($t_{1/2}=3.2\pm0.4$ s) and $0.12\pm0.01\ s^{-1}$ ($t_{1/2}=5.8\pm0.6$ s), respectively, averaged over the six runs. Pressure units are in Torr. Initial total pressures are represented by P_0 and the pressure increases after total FOOF/FOO decomposition are given by ΔP. Initial integrated areas of the FOOF and FOO bands at 1210 cm^{-1} and 1490 cm^{-1}, respectively, are given by the A_0 values.

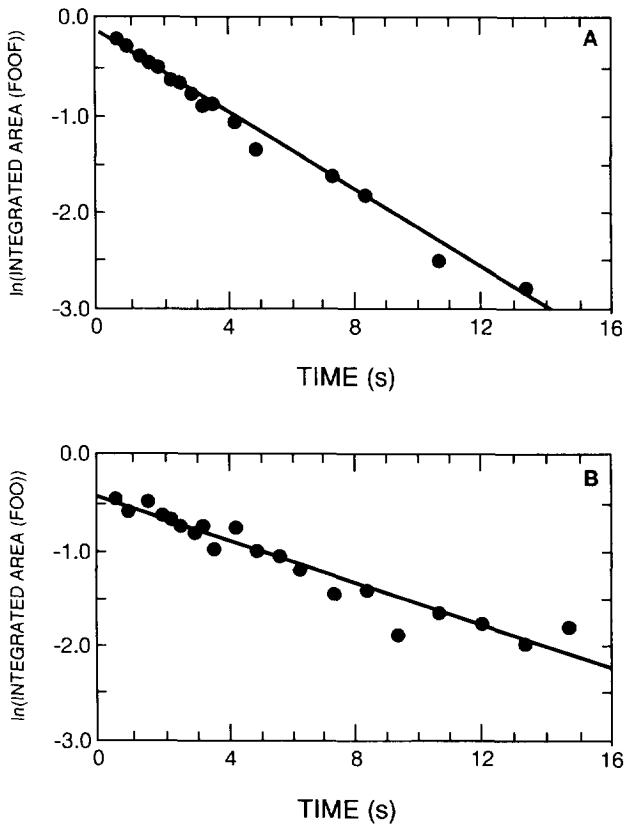

Fig. 5. Typical first-order kinetic plots for (A) the disappearance of the FOOF absorption envelope centered at 1210 cm^{-1} and (B) the disappearance of the FOO absorption envelope centered at 1490 cm^{-1}.

5.8 s) was obtained from an average over the same six runs. The error limits reported are the standard deviation of the average of the six kinetics runs.

3.4. Photolysis experiments

Fig. 6 shows the infrared spectrum that resulted when a circulating gas mixture consisting of 300 Torr each of O_2 and F_2 at ambient temperature was irradiated with a high-pressure Hg/Xe lamp upstream of the infrared cell [2]. In this experiment, the transit time between the irradiation zone and the infrared cell was several seconds or less. The formation of FOO is clearly indicated by characteristic absorption features near 1490 and 600 cm^{-1}. Significantly, there were no detectable absorptions for FOOF. The measured FOOF absorption coefficient was used to estimate an upper FOOF concentration limit of <0.01 Torr. By applying the absorptivity value for FOO derived above, it is calculated that the partial pressure of this species in the infrared cell was ≈ 0.2 Torr.

3.5. FT-IR experiments with O_2 carrier gas

Fig. 7 shows the results obtained from a typical set of ambient-temperature flow experiments in which 'batch' FOOF was carried into the FT-IR cell by a driving pressure of gaseous O_2. The O_2 pressures complemented those in runs represented by Fig. 2 (no added O_2) and Fig. 6 (300 Torr O_2, photolysis). Fig. 7 clearly shows that high O_2 pressures favored the conversion of FOOF to FOO. Significantly, Fig. 7 also shows that, even at a relatively high ratio of O_2 to FOOF, this conversion was far from complete. These observations strongly support earlier suggestions that, in the gas phase, O_2 reacts directly with FOOF to form FOO — possibly in an equilibrium process, as depicted by reaction (6) [5,6]:

$$FOOF + O_2 \rightleftharpoons 2FOO \qquad (6)$$

If equilibrium conditions [reaction (6)] were achieved in our FOOF/FOO decomposition experiments (with and without O_2 carrier gas), a plot of $[FOOF][O_2]$ versus $[FOO]^2$ should be linear with a slope equal to K_{eq} since the equilibrium expression may be written as:

$$K_{eq}[O_2] = [FOO]^2/[FOOF] = E(A_{FOO})^2/A_{FOOF} \qquad (7)$$

The A quantities are infrared absorbances and $E = (\epsilon_{FOOF})/b(\epsilon_{FOO})^2$, where the ϵ terms are infrared absorption coefficients and b is the pathlength. Fig. 8 depicts a plot of the FOOF concentration multiplied by the O_2 concentration

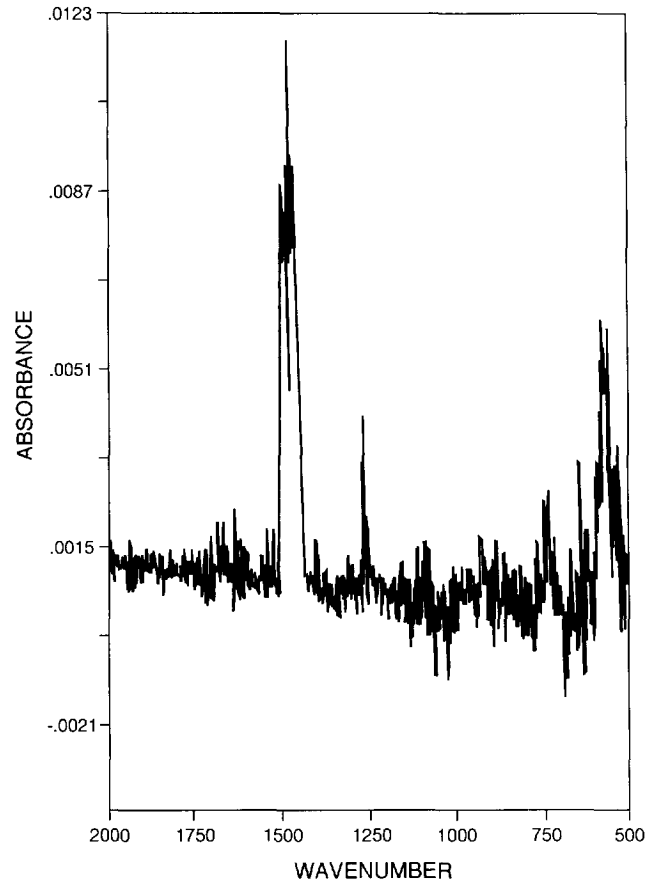

Fig. 6. The infrared spectrum which resulted when a flowing gas mixture containing 300 Torr each of O_2 and F_2 (ambient temperature) was irradiated with the output of a high-pressure Hg/Xe lamp. The lamp output was filtered by a water-filled quartz cell.

[2] The photochemical quantum yield is approximately unity for the generation of FOOF in liquid O_2/F_2 [18]. The quantum yield for FOO generation by photolysis of gaseous O_2/F_2 mixtures is also near unity [6].

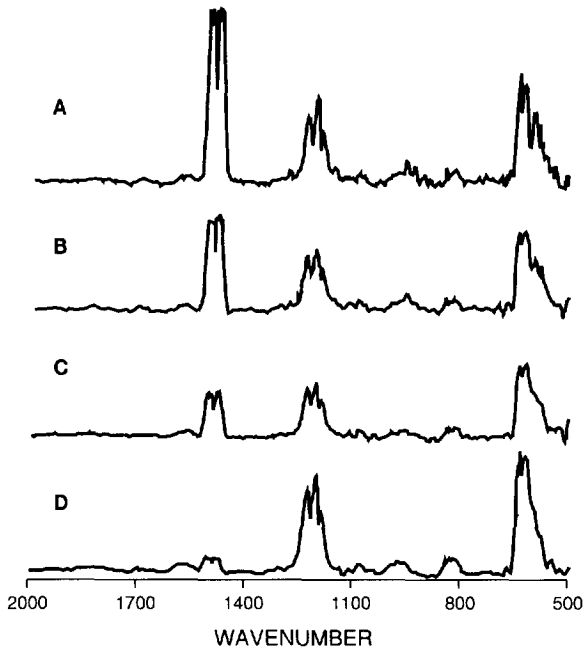

Fig. 7. The infrared spectrum of flowing FOOF/FOO gas mixtures in the presence of O_2 carrier gas at ambient temperature. Nominal pressures: (A) 310 Torr O_2, 20 Torr FOOF; (B) 133 Torr O_2, 12 Torr FOOF; (C) 38 Torr O_2, 13 Torr FOOF; (D) 0 Torr O_2, 12 Torr FOOF. The absorbance scales are identical for each spectrum.

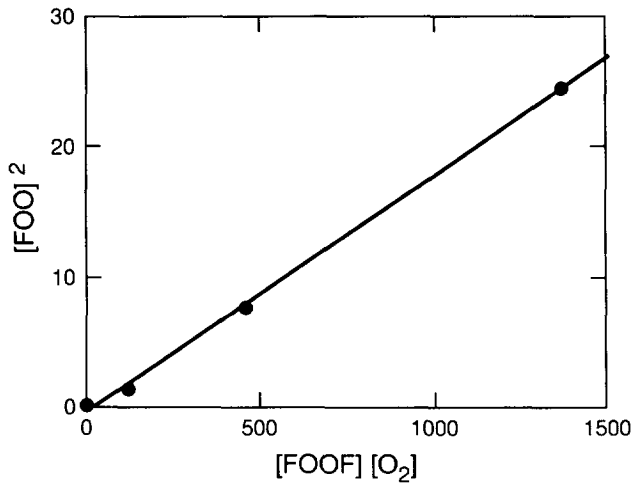

Fig. 8. Equilibrium plot fr the FOOF/FOO/O_2 system where the concentrations are expressed in Torr and have been calculated using the peak heights of FOOF and FOO with their respective absorptivities.

versus the square of the FOO concentration. The concentrations were calculated from the intensity (peak height) data by using the calculated peak absorptivities. Fig. 8 shows that the plot is linear over a large pressure range and yields an equilibrium constant of 0.018 at 297 K. A value of 0.046 at 286 K has been reported previously on the basis of a more restricted set of data [5]. These values are much larger than the equilibrium constant calculated from the reported free energies of formation for FOOF (13.9 kcal mol^{-1}) and FOO (8.8 kcal mol^{-1}) at 300 K [19]. However, these free energies may be subject to errors of 1–2 kcal mol^{-1} and the discrepancy between measured and calculated equilibrium constants may be more apparent than real [20]. The linear plot in Fig. 8 suggests that equilibrium was established near ambient temperature more rapidly than the decomposition of either FOOF or FOO. An additional significant observation is that, at high oxygen and FOOF/FOO pressures [e.g. Fig. 7(A)], the half-lives for the decomposition of both FOOF and FOO appear to be much shorter. In fact, the initial reactions were too rapid to measure conveniently with the experimental set-up used in this study. When the FOOF/FOO pressures decreased, the rates of decomposition also decreased. It is apparent that under high-pressure conditions the decomposition kinetics decidedly do not obey simple first-order behavior as described for the preceding EPR and FT-IR experiments, which were carried out at much lower pressures.

4. Discussion

Our observed first-order rate constant for the overall decomposition of FOOF at ambient temperature [reaction (1)] is $0.22 \pm 0.03\ s^{-1}$. Another value ($1.2\ s^{-1}$) reported for this reaction is that of Schumacher and Frisch [8]. Because this number is the result of an extrapolation of pressure data obtained in 1937 at low temperature for decomposing 'batch' FOOF amidst formidable material and handling difficulties, we feel the comparison with our value is reasonable. Campbell's reported data were taken at ≈ 286 K and much lower pressures, at which wall reactions were minimized; from these data an approximate rate constant of $0.02\ s^{-1}$ can be derived [5e]. Considering the differences in experimental details, the agreement with our result is reasonable.

Previous determination of the overall ambient-temperature decomposition kinetics of FOO [reaction (2)] is apparently limited to the work of Chegodaev and coworkers [7] and the more comprehensive work by Lyman and Holland [6]. Lyman and Holland proposed that, at relatively high total pressures (low FOO partial pressure), the reaction is second-order in FOO with an upper limit of 33 l mol^{-1} s^{-1} as the homogeneous rate constant; this limit is somewhat dependent upon third-body gases [6]. The derivation of rate constants for the overall FOOF/FOO decomposition does not by itself afford insight into any possible decomposition mechanisms: in addition to reactions (1) and (2) direct irreversible decomposition of FOOF/FOO to F_2 and O_2), reaction (6) and sequences such as reactions (8)–(10) should also be considered. Researchers have previously suggested that some of these reactions are important in the FOOF/FOO decomposition [2,5–7].

$$FOOF + FOOF \longrightarrow 2FOO + F_2 \quad (8)$$

$$FOO \longrightarrow O_2 + F \quad (9)$$

$$2F \longrightarrow F_2 \quad (10)$$

Such reactions are known (or are suspected) to be influenced strongly by third-body wall and gas effects.

A simple decomposition mechanism based predominantly upon the sequence of reactions (8)–(10) can be discounted for several reasons: (a) the kinetic data are first-order instead of second-order in FOOF; (b) this sequential mechanism does not allow for the observed effects of O_2 {i.e., the change in rate and the shift from first to second order with increasing O_2 pressure [reaction (6)]}; (c) thermodynamic and kinetic considerations overwhelmingly favor the *reverse* of reaction (9) [6]; (d) the well-known sluggishness of fluorine-atom recombination [reaction (10)] suggests that F atoms should have been detected readily in the EPR experiments if F atoms were involved in this decomposition pathway [6]; and (e) if only sequential reactions of the type described above occur, a build-up in the concentration of FOO would have been expected sometime after FOOF was injected into the kinetic cell. Using the sequence of reactions (8)–(10) as a model and the experimentally derived FOOF and FOO decomposition rate constants, the calculated time-dependent concentration profiles for FOOF and FOO indicate that the FOO concentration should reach a maximum at ≈ 5 s for a typical set of experimental conditions. Extensive analysis of all our data showed that such an induction period was not observed on the time scale of our experiments.

Another possible reaction sequence consists of a rapid pre-equilibrium [reaction (11)] and rapid F-atom scavenging by the reverse of reaction (9), accompanied by direct irreversible decomposition of FOOF [reaction (1)] and/or FOO [reaction (2)] as the rate-determining step:

$$\mathrm{FOOF} \rightleftharpoons \mathrm{FOO} + \mathrm{F} \qquad (11)$$

This sequence allows for the appearance of FOO in FOOF gas streams without a build-up in FOO concentration, and correctly predicts the observed FOOF reaction order and the predominance of FOO (relative to FOOF) in the presence of excess oxygen. However, this mechanism fails to account for the apparent dependence of the rate law on the O_2 pressure. Also, under our conditions, the thermodynamics of reaction (11) in the forward direction would have been so highly unfavorable that only FOOF should have been observed if only these reactions were operative [19] [3].

The critical observations that allow us to infer a possible mechanism for FOOF/FOO decomposition are the FOOF/O_2/FOO equilibrium [shown in Reaction (6) and discussed above], and the FOOF/FOO reaction that changed from first order at low O_2 concentration to higher order at high O_2 concentration. Other relevant facts are that the first-order rate constant for the disappearances of FOOF, k_{FOOF} (Table 1), is independent of O_2, F_2 and FOO pressures (as long as P_{O_2} is relatively low) and that the apparent first-order rate constant for the disappearance of FOO at low P_{O_2} is slower than that of FOOF by a factor of ca. 2. These facts suggest that the equilibrium depicted in reaction (6) is rapid not only on the time scale of FT-IR absorbance measurements at the FOOF/FOO concentrations described above, but also on the time scale of the decomposition kinetics. Thus, the first-order kinetics (in FOOF) at low P_{O_2} occur because FOOF is the predominant species and, accordingly, the kinetics are carried by the first-order decomposition of FOOF. At high P_{O_2}, on the other hand, FOO is the major species and the decomposition of FOOF/FOO is carried by a reaction that is bimolecular in FOO, as is shown schematically below:

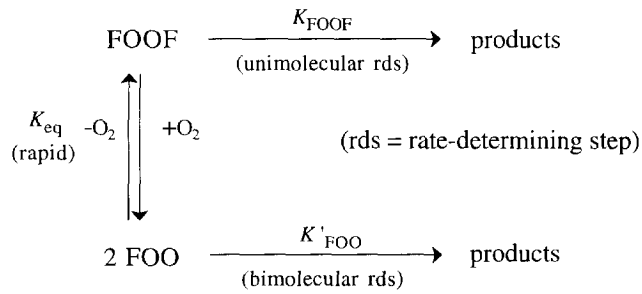

The insensitivity of k_{FOOF} to the parameters noted above and also to the total gas pressure suggests that the rate-determining step at low P_{O_2} is a unimolecular decomposition process. The rate constant is, however, somewhat dependent upon the surface, which suggests that at least part of the FOOF decomposed on the cell walls. The reaction product of the unimolecular rate-determining step cannot be gas-phase FOO because this species would then build up as noted above in the discussion of the essential process [reactions (8)–(10)]. Therefore, a tenable homogeneous process corresponding to the k_{FOOF} step is the direct decomposition of FOOF to F_2 and O_2. Such a process might be facilitated by large-amplitude, highly anharmonic motions involving both torsion about the F–O–O–F dihedral angle and a bending of the O–O–F angles. Strong overtone and combination tones were observed in the infrared spectra, suggesting large anharmonicities in these motions [9].

At low P_{O_2}, the decomposition of FOO appears to be first order and the rate constant k'_{FOO} is approximately one-half of k_{FOOF} (vide supra). The apparent first-order behavior is easily understood because at low P_{O_2} the overall decomposition reaction is carried by k_{FOOF}, and FOO decomposes by first being converted to FOOF by the rapid pre-equilibrium represented in K_{eq}. The magnitude of k'_{FOO}, however, is initially surprising: the stoichiometry of the above scheme appears to dictate $k_{FOO} = 2k_{FOOF}$. Nonetheless, O_2 is a product of the decomposition and P_{O_2} increased during the course of the reaction. Accordingly, the FOO/FOOF ratio will increase as P_{O_2} increased during the process of the reaction as a result of the FOOF/FOO/O_2 pre-equilibrium. Hence, at low P_{O_2} relative to the rate of disappearance of FOOF, FOO decomposition must be slower than simple stoichiometry would suggest.

At high P_{O_2}, FOO is the dominant oxygen fluoride species and the overall decomposition reaction is carried by the bimo-

[3] Note, however, that the thermodynamics of FOOF and FOO are not known precisely and consequently this argument is subject to some uncertainty.

lecular decomposition of FOO, represented by k'_{FOO} in the above scheme. We have not studied this reaction as thoroughly as the reaction at low P_{O_2}, and thus we have not established the dependence of this reaction upon F_2, O_2, third bodies, etc. However, some mechanistic conclusions can be drawn. The product of the rate-determining step cannot be FOOF; like the reverse reaction in the pre-equilibrium step, this would result in a build-up of FOOF and, ultimately, would limit the overall reaction rate by k_{FOOF}, which clearly was not the case at high P_{O_2}. The most likely reaction for the bimolecular rate-determining step in the decomposition of FOO is direct formation of F_2 and O_2 via an OOF — FOO collision. This reaction is probably facilitated by third-body gas or wall collisions.

As noted above, an upper limit on the homogeneous rate constant for the bimolecular decomposition of FOO was estimated as 33 l mol^{-1} s^{-1} at ambient temperature (derived from Ref. [6]). The boundary conditions for the reaction scheme described above require $k'_{FOO} > 10^3$ l mol^{-1} s^{-1}. Although our reaction conditions differed greatly from those of Lyman and Holland [6] and third-body effects on the homogeneous reaction could not be excluded, it is likely that a homogeneous reaction contributed to the complicity of our experiments.

Based upon the above arguments, the most probable mechanism is given in the expanded scheme below:

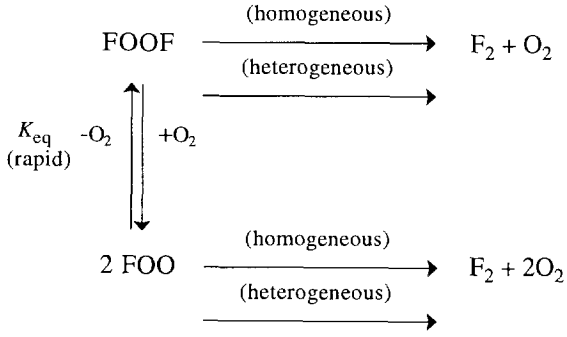

The facts suggest that the heterogeneous pathway is a significant but not dominant pathway for the decomposition of FOOF, whereas the heterogeneous reaction may be dominant for FOO decomposition.

In earlier work, Campbell and Kim [5c] studied the decomposition of FOOF/FOO at low pressures ($\approx$100 mTorr) and low temperatures in a large-diameter cell where wall collision frequencies were minimal compared to those in our apparatus. They showed that, at their temperatures (160–270 K) and in their system, wall reactions were relatively unimportant. Lyman and Holland [6] have extensively investigated the gas-phase formation and decomposition rates of FOO and FOOF at low partial pressures (high carrier gas pressure) and ambient temperature under conditions in which wall collisions were again insignificant. They observed second-order FOO decomposition rates and some dependence upon the third-body gases [4]. If only Lyman and Holland's second-order FOO rate constants are used to model the overall homogeneous decomposition of FOOF/FOO, the predicted kinetic stability of FOOF/FOO is far greater than that observed in our experiments. Diffusion calculations indicate that with a geometry and pressure typical to our experiments, a wall reaction probability of only about 0.09% per collision is necessary to roughly model our data [19]. This conclusion applies only to the bimolecular reaction involving FOO, and not to the low-P_{O_2} regime in which unimolecular decomposition of FOOF is dominant.

Our results reflect the operative mechanism for FOOF/FOO decomposition under a relatively limited set of experimental conditions, and therefore our rate constants and mechanistic conclusions must be regarded as similarly limited [3]. Initially, in 'batch' FOOF experiments, *only* FOOF is present so direct decomposition not involving O_2 *must* occur — presumably by third-body reactions [reaction (1)] as previously postulated [6]. At intermediate times, the O_2 concentration is rapidly changing and is comparable to the FOOF/FOO concentrations. Near the end of the reaction, the O_2 concentration is high and essentially constant, a situation also extant for the O_2 carrier and photolysis runs. The effect of the increasing oxygen concentration as 'batch' FOOF decomposes is to shift the equilibrium shown in reaction (6) to the right and thereby enhance pathways that involve direct FOO decomposition [reaction (2)]. Because the source terms for decomposition (FOOF and/or FOO) are constantly changing as a result of equilibrium in reaction (6) and others, simple first- and/or second-order expressions cannot fully describe the actual kinetics if the above mechanism is correct. Nevertheless, careful examination of our experimental data shows that the above hypothesis is self-consistent and reasonable for the pressure range over which decomposition rates were studied.

A final point is pertinent to the preceding discussion: FOO (especially in the low-pressure runs) could originate partially from the FOOF supply itself because higher oxides such as O_4F_2 can be produced during synthesis and these oxides dissociate to FOO in the liquid state [2]. However, if this were the source of a significant amount of FOO, then we should have observed fractionation (i.e., changing FOOF/FOO ratios) in the gas stream as the FOOF supply cylinder was depleted because of the well-known poorer stability of O_4F_2. Because no such effect was observed, this possibility seems remote. In addition, Raman studies of solid and liquid FOOF have revealed only very small quantities of FOO in the condensed phases [9].

A second possibility is that FOO was generated as the FOOF vaporized and exited from the supply cylinder.

[4] In Lyman and Holland's study, reaction (11) and the reaction FOO + FOO → F_2 + O_2 are very important in determining the overall decomposition rate. Because their calculated F-atom concentration is well below the upper limit set by our EPR studies, this mechanism is consistent with our results.

Because of the way in which the FOOF supply cylinder was warmed and FOOF was delivered to the cell, it is conceivable that there was a significant residence time in the supply cylinder at pressures higher than in the FT-IR cell and at temperatures high enough for significant FOOF decomposition to occur. However, numerous experiments with Dry-Ice cooling of the transfer lines and the upper part of the FOOF supply cylinder gave no evidence that this occurred to any appreciable extent.

5. Conclusions

EPR and FT-IR spectroscopy have been employed to follow the decomposition of FOOF and FOO in the gas phase by using flow and stopped-flow systems. The concentration of F atoms in FOOF/FOO that underwent decomposition at total pressures below 5 Torr was below the EPR detection limit of 5×10^{-3} Torr. The evolution of oxygen in the decomposition reaction followed approximate first-order kinetics, and the measured rate constant was somewhat dependent upon the wall materials. The FT-IR data at low P_{O_2} showed that the FOOF/FOO decomposition is first order with rate constants compatible with the rate of evolution of O_2 as determined by EPR under similar conditions. At high P_{O_2}, second-order decomposition of FOO/FOOF was observed. It is likely that a decomposition mechanism occurs that involves a rapid pre-equilibrium between FOOF and O_2 to yield FOO, and that unimolecular FOOF decomposition or bimolecular FOO decomposition is the rate-determining step — depending upon whether FOOF or FOO is the dominant species, as determined by P_{O_2}.

Acknowledgments

This work was supported by the US Department of Energy, Office of Nuclear Materials Production. M.P. Eastman was an Associated Western Universities Faculty Participant at the Los Alamos National Laboratory. Partial support of M.P. Eastman while he was a faculty member of the University of Texas at El Paso by the Robert A. Welch Foundation of Houston, Texas is gratefully acknowledged. We also thank Drs. R.C. Kennedy, K.C. Kim, and especially J.L. Lyman of the Los Alamos National Laboratory for many useful discussions and suggestions.

References

[1] I.V. Nikitin and V.Y. Rosolovskii, *Russ. Chem. Rev., 40* (1971) 889.
[2] A.G. Streng, *Chem. Rev., 63* (1963) 607.
[3] J.G. Malm, P.G. Eller and L.B. Asprey, *J. Am. Chem. Soc., 106* (1984) 2726.
[4] L.B. Asprey, S.A. Kinkead and P.G. Eller, *Nucl. Technol., 73* (1986) 69.
[5] (a) K.C. Kim and G.M. Campbell, *J. Mol. Struct., 129* (1985) 263; (b) K.C. Kim and G.M. Campbell, *Appl. Spectrosc., 39* (1985) 625; (c) K.C. Kim and G.M. Campbell, *Chem. Phys. Lett., 116* (1985) 236; (d) G.M. Campbell, *J. Mol. Struct., 189* (1988) 301; (e) G.M. Campbell, *J. Fluorine Chem., 46* (1989) 357.
[6] J.L. Lyman and R. Holland, *J. Phys. Chem., 92* (1988) 7232.
[7] (a) P.P. Chegodaev, V.I. Tupikov and E.G. Strukov, *Russ. J. Phys. Chem., 47* (1973) 746; (b) P.P. Chegodaev and V.I. Tupikov, *Dokl. Akad. Nauk SSSR, 210* (1973) 647.
[8] H.J. Schumacher and P.Z. Frisch, *Z. Phys. Chem., B37* (1937) 1.
[9] R.C. Kennedy and T.R. Mills, unpublished results.
[10] K.O. Christe, C.J. Schack and R.D. Wilson, *Inorg. Chem., 15* (1976) 1275.
[11] E.M. Larson, W.H. Woodruff, P.G. Eller, B.I. Swanson, S.A. Kinkead and L.H. Jones, Paper presented at the American Chemical Society National Meeting, Denver, CO, April 1987.
[12] A.A. Westenberg and N. DeHass, *J. Chem. Phys., 40* (1964) 3087.
[13] N.M. Atherton, *Electron Spin Resonance,* Halsted Press, New York, 1973, p. 397.
[14] (a) N.J. Lawrence, J.S. Ogden and J.J. Turner, *J. Chem. Soc. A,* (1968) 3100; (b) F.E. Welsh, F.I. Metz and W.B. Rose, *J. Mol. Spectrosc., 21* (1966) 249; (c) F.J. Adrian, *J. Chem. Phys., 21* (1967) 1543, and references cited therein.
[15] (a) A. Carrington, D.H. Levy and T.A. Miller, *J. Chem. Phys., 45* (1966) 4093; (b) D.E. Radford, V.W. Hughes and V. Beltram-Lopez, *Phys. Rev., 123* (1961) 153.
[16] D.R. Stull and H. Prophet, *JANAF Thermochemical Tables,* 2nd edn., US Department of Commerce – US National Bureau of Standards, Washington, DC, 1971.
[17] (a) V.S. Arutyunov and A.M. Chaikin, *Kinet. Katal., 18* (1977) 316; (b) V.S. Arutyunov and A.M. Chaikin, *Kinet. Katal., 18* (1977) 321.
[18] P.G. Eller and S.A. Kinkead, unpublished results.
[19] J.L. Lyman, *J. Phys. Chem. Ref. Data, 18* (1989) 799.
[20] J.L. Lyman, personal communication.